

We would like to thank the editor and all reviewers for their feedback and suggestions that helped to improve the manuscript. All reviewer comments, our responses and the changes made in the manuscript are summarised below. Changes made to the manuscript are shown in blue. References to the position of these changes in manuscript have been updated to the position in the revised manuscript. Tracking of revision is appended to this summary.

### **Response to Reviewer Comment #1**

Response to general comment on model comparison is given below under Comment no. 13. Here we will focus on the content-related comments by the referee. Criticism of linguistic quality caused us to repeat and extend our proof-reading procedure (see revision tracking below).

Response to detailed comments:

1. “Page 3, line 20 ~~30~~: The computational demands of semi-distributed models with polygon based delineation is nowadays often negligible.”

We agree that the computational demand to perform a single model run is often negligible, but this omits the demands for model calibration or extensive sensitivity analysis studies. However, the actual formulation does not address this subjects and has been reformulated as follows:

“The aim of the proposed algorithm is set to offer a basin partition with a minimum of heterogeneity by a minimum of sub-divisions, i.e. to ~~reduce the computational calibration effort the~~ number of unnecessary sub-divisions and subsequently the number of parameters in cases of hydrological modelling.”

*[Page 3, Line 30]*

2. “Page 4 and Fig. 2: Pore volume and available water capacity should be defined. For instance is with “total pore volume” the “porosity” meant? Usually these variables are given in volume percent? Here they are given in mm, why? Does this not require an information about the soil depth?”

Our data basis provides the opportunity to assess soil properties in different depths. In previous projects, where this data has been applied, we experienced that the majority of soil storage is located in the upper zones of the soil layer. Namely a depth of up to 2 meters covers nearly all available soil storage. Why we applied the *[mm]* data and not the [%] is in this case due availability (data from previous project) than for any particular consideration.

The employed TPV data is calculated for a soil depth of up to 2 meters, this information has been added to the manuscript, Legend in Figure 2 and Page 4 Line 18-19 have been revised:

“To characterise the soil characteristics of the German catchments, a gridded soil data map from the German Federal Institute for Geosciences and Natural Resources (BÜK200) and CORINE land coverage data (CLC) (Bossard et al., 2000) were used. Pedo-transfer functions (Sponagel, 2005) were applied to transfer this information into gridded data about (available) water capacities (AWC), **maximum soil**

storage capacity (referred as total pore volume TPV) and hydraulic conductivity (HC) for the upper soil, up to two meters depth.”

[Page 4, line 32]

- “Page 5, Lines 24-25: I was trying to picture the basin split into stripes. I found Figure 5 as an visual explanation. However, comparing Fig. 5 with Fig. 3 there should be much less points of the distance-factor function in Fig. 3 (only 5 points). Later I realised that Fig. 3 does not belong to Fig. 5. For demonstration purpose I would suggest providing a pair of Figures with distance classes and corresponding distance factor function using a few classes only. May be Fig. 5 needs to come before Fig. 3.”

The enhance comprehensibility we follow your recommendation. The distance-factor function of the synthetic catchment has been created (see Figure below) and added to the manuscript as Fig. 4. The synthetic catchment is now introduced on *Page 6, Line 19* as follows:

“Please note that  $w(x)$  is the non-normalised value of the area-function (Snell and Sivapalan, 1994). To visualise the proposed function a simple synthetic basin with its stream network, distance-classes and an arbitrary characteristic is shown in Fig. 3. To keep things simple Fig. 3c shows the unified flow length (comprising  $x_S$  and  $x_H$ ) derived from the flow direction data in Fig. 3b. As it can be seen in Fig. 3c the basin has been split into 5 distance classes. Applying Eq. 1 and 2 to the data (Fig. 3a) produces the average and standard deviation within these five distance classes. The obtained distance-factor function is shown in Fig. 4.

Figure 5 shows the application to real data in a meso-scale catchment, namely for AWC in the Mulde catchment.”

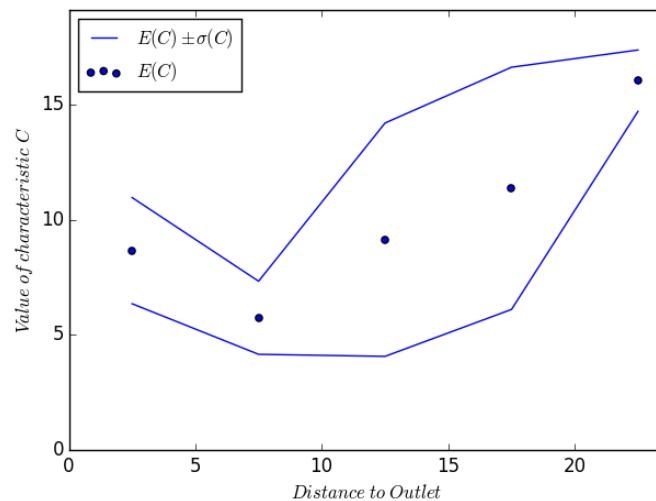


Figure 3: Distance-factor function of sample Data in synthetic catchment

- “Page 5, line 31: (Eq. 1 and 2)“

Already addressed in previous point.

- “Fig. 4: Use the same units on the x-axis as in Fig. 3.”

Figure 4 (now 5) has been revised.

6. “Fig. 5: Example input data are on the “left”!”

Subscript of Fig. 5 (now 3) has been changed as noted.

7. “Page 12, Eq. 8: I would suggest to explain this equation in words. I also would suggest to exchange the sides of omega and sigma (even if mathematically not necessary) in both numerator and denominator.”

We suppose the suggestion to switch omega and sigma is indented to clarify the summation. Instead of switching the summands we added parenthesis for clarification. An explanation of Eq. 9 has been added to the manuscript on *page 13, line 4*:

“In addition to this we applied a second performance metric to evaluate to what extend our target has been met. The metric  $\alpha_2$  highlights cases where the total heterogeneity was decreased significantly, however, but still being above objective as defined by threshold  $\Omega$ . The metric  $\alpha_2$  was calculated as the delta between threshold  $\Omega$  and standard deviation in the separated catchment  $\sigma_S(C)$ , normalised by the delta between  $\Omega$  and the standard deviation in the unseparated catchment  $\sigma_U(C)$ :

$$\alpha_2 = \frac{\sum_{i \in M(S)} (\Omega - \sigma_{S,i}(C))}{\sum_{j \in M(U)} (\Omega - \sigma_{U,j}(C))} \quad (9)$$

8. “Page 12, line 15: What are cases with “negative outcome”? Do you mean insufficient variance reduction?”

That is correct. Page 13, line 21 has been revised as suggested:

“Focussing on cases with **insufficient variance reduction** we were able to identify some limitations for the algorithm”

9. Fig. 8, 9 and 12: The distance factor functions are hard to read. Use vector graphics and/or large fonts and/or larger figures.

Figures have been revised. Figures are now embedded in EPS format, fonts have been enlarged. Figures will be submitted separately for better processing.

10. “Fig. 10: In the legend of AWC “max” and “min” need to be exchanged.”

Legend of Fig. 11 has been revised.

11. Fig. 11: When resampling of AWC for the Mulde river basin is shown also the original AWC map of the Mulde basin should be shown for comparisons. Why are there some kind of horizontal stripes in Fig. 11?

The map of original AWC values in the Mulde basin is not shown in the manuscript, because the spatial arrangement of AWC and the shown TPV is identical (as mentioned on *page 14, line 24*) due to origin of these data grids. Both values follow the arrangement of the soil map, their only difference is the range of values (also given in *line 24*), caused by different calculation formula (Sponagel, 2005). Since the manuscript already has a great number of figures and the information content of the AWC figure low we omitted it in the original manuscript.

The stripes in Fig. 11 (now 12) are caused by the process of quantile exchange. In Fig. 2 it is visible that on a small scale the variance of the characteristic is in comparison to the total variance very low. When these values are transferred to their empirical quantile, their numbers differ only from the fifth or sixth digit. A reduction of digits and the application to another empirical distribution function, with values that are again rounded, resulted in the visible stripes.

We are very thankful for this review comment since it pointed out a problem that got lost along the way of preparing this manuscript. We revised and re-applied the resampling scheme, with the results that we were able to remove the stripes (see revised Fig. 12). Changes in the input to sub-basin ascertainment led to slightly different results (rev. Fig. 13) and performances compared to the initial results. However, altered results do not lead to different conclusions.

**Table 1: Normalized reduction of standard deviation for resampled basins**

Catchment	Pore Volume		Slope	
	$\alpha_1$ [%]	$\alpha_2$ [%]	$\alpha_1$ [%]	$\alpha_2$ [%]
Mulde (res)	58.9	26.2	8.9	76.4
Salzach (res)	39.7	4.8	19.7	37.5

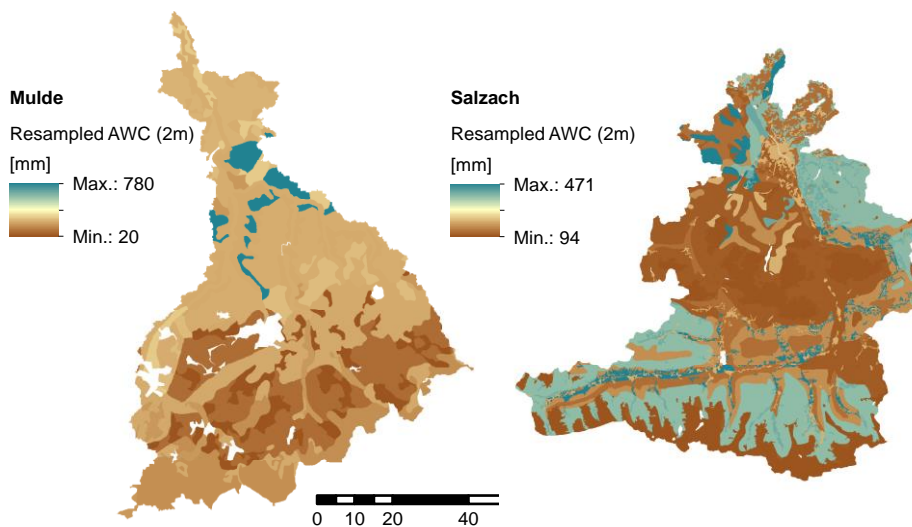


**Figure 12: Resampled AWC values for Mulde and Salzach catchment**

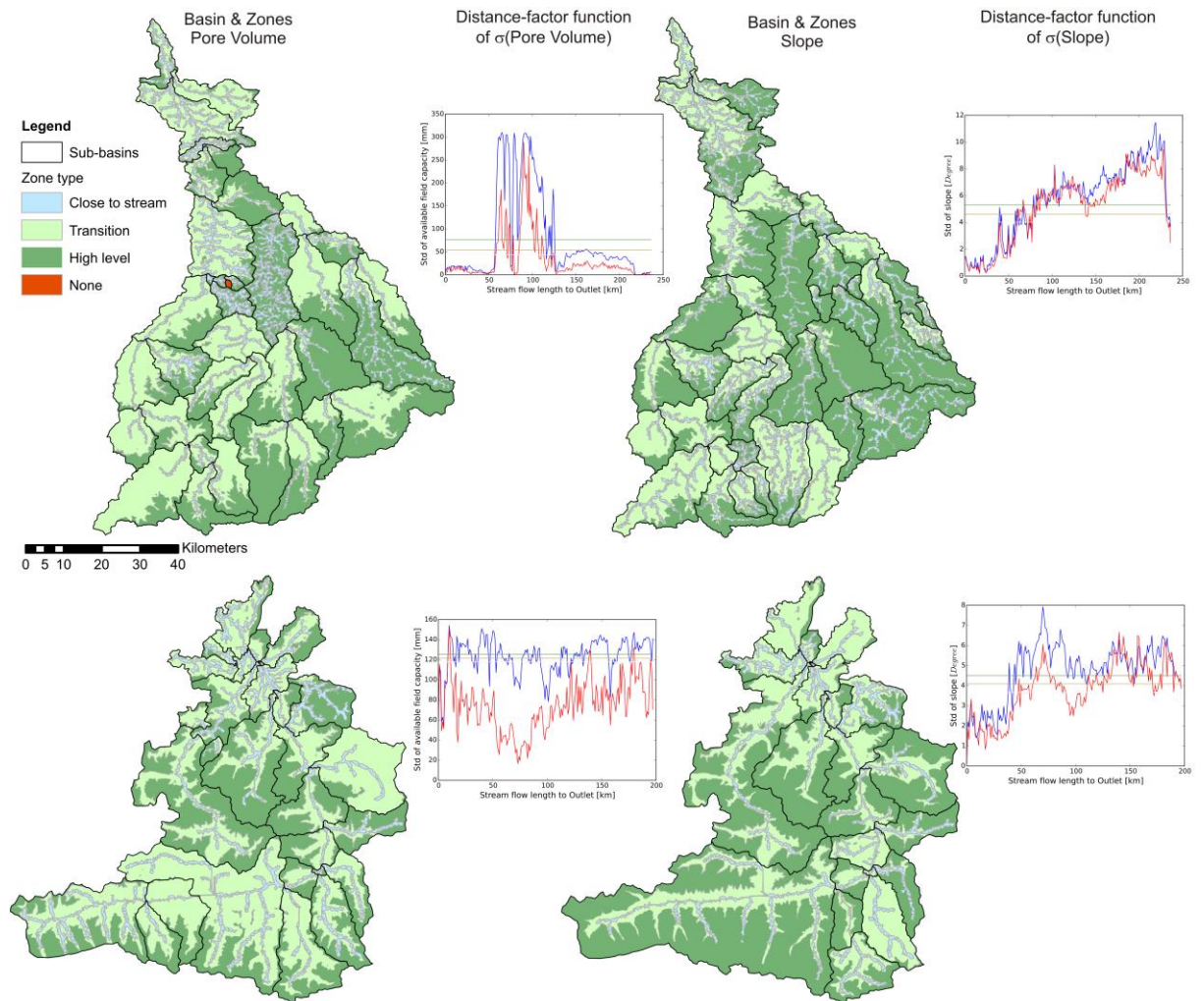


**Figure 13: Results of ACS application for resampled catchments of the Mulde and Salzach (from top to bottom), sub-basins based on resampled pore volume (left) and slope (right). Comparison of  $\sigma_u(C)$  and  $\sigma_s(C)$  for each application (red and blue lines).**

Changed results have been transferred to the manuscript as on *page 15, line 13*:

“We also experienced a change in performance for the slope. The exchange of heights values led to a lower range of slope values and a lower amount of heterogeneity. These patterns resulted in all other applications in inferior  $\alpha_2$  performances. Still, the geomorphologic structure of the basin remained unchanged and heterogeneity could be assessed by the algorithm (visible through unchanged total reduction).”

12. “Page 16, line 29, Table 4: Where are the 30 different zones per sub-basin coming from; why so many; how are these zones defined?”

In this section the partition by land cover and heights from Sec. 5.1 is converted into a model structure. As indicated, this separation scheme follows the recommendations by Lindström et al. (1997): Land cover to account for soil and heights for precipitation and evaporation correction factors. Land use has been divided into forest (all types), bare soil/rock and field (all remaining cells that are not water). Threshold for heights partition has been set to 100m. The obtained spatial setup is shown in Fig. 13 & 14.

Choice of 100m as height threshold is due to the usage in the original HBV publication by Bergström (1976) who used a similar heights subdivision (900m / 10 height-zones) and the HBV model of the German Federal Institute of Hydrology which has been applied in a project at our institute (<http://doi.bafg.de/BfG/2016/BfG-1877.pdf>).

13. “Page 17, Table 5: As already mentioned in the general comments the comparison of the performance for two model versions with such a large difference in number of parameters needs to be given some more thought. Could the reason for the better model performance not be just because of the smaller number of parameters and therefore the smaller complexity and easier calibration. This might be tested by an additional model version using the same small number of parameters as in the new delineation scheme but applied on the old conventional basin separation (using only 3 zone per sub-basin too)?”

The trade-offs between parameters and model performance are a topic for themselves and we intended to address it just as scantily as possible. Therefore, we tried to stay consistent in our modelling choices. We applied the same basin partition schemes that we applied in the previous sections and used the same parameter coupling scheme. Parameter coupling included only 6 zonal parameters, all remaining zonal parameters were due to calibration. Our decision for consistency resulted in the shown number of parameters for the three models.

On the one hand we agree with your statement that more parameters make the model more complex which could lower the model performance. On the other hand, a higher number of free parameters offers more flexibility to fit the observed behaviour. We expected that a model with more parameters would perform better than the parsimonious setup in the calibration period. Due to the high degree of specialisation (fitted model parameters) we expected a greater loss of accuracy for high parametrised model structures than for the parsimonious. Our results so far show that even in the calibration period the performance of the parsimonious setup is superior. Leading to our conclusion that the advantage of more flexibility, even with the same parameter coupling scheme, does not compensate the value of the information we added to the model. We closed our analysis at this point because we defined our benchmark as the “common” scheme for the HBV<sub>96</sub> model.

However, as your comment pointed out, we did not consider a benchmark model with a comparable number of parameters but with different spatial resolution. We suggest to stick with the benchmark basin partition scheme and extend the coupling scheme. Previously, parameters that could be somehow reasonably be related to storage information (like SM – soil storage, ICMAX – interception storage etc.) were coupled between the zones within a sub-basin. When we loosen this restriction and take all parameters into the coupling scheme we are able to reduce the number of free parameters (see Tab. RS1). This advanced coupling scheme has been applied to the ACS model as well to gain comparability of calibration effort.

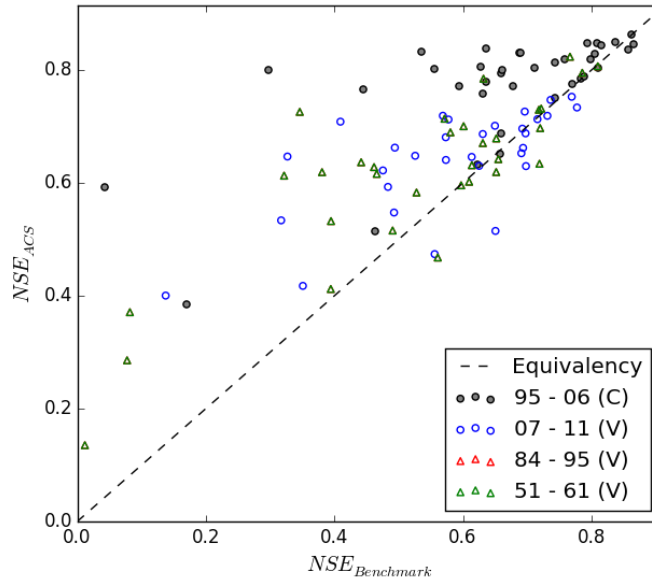
**Table 4: Parameter quantities**

	Benchmark <i>Free</i>	Benchmark <i>6-Coupled</i>	Benchmark <i>All coupled</i>	ACS <i>6-Coupled</i>	ACS <i>All coupled</i>
Sub-basins	38	38	38	44	44
Zones per Sub.	~30	~30	~30	3	3
Parameter (total)	19562	12198	1710	2244	1980
Parameter (per Sub.)	~495	~321	45	51	45

Evaluation of the new calibration schemes gives the following results:

**Table 5: Nash-Sutcliffe Efficiencies of Benchmark and ACS-model**

Simulation (Start-End)	$NSE_{B:Free}$ [-]	$NSE_{B:6}$ [-]	$NSE_{B:All}$ [-]	$NSE_{ACS:6}$ [-]	$NSE_{ACS:All}$ [-]
1995 - 2006 (C)	0.678	0.659	0.682	0.792	0.791
2007 - 2011 (V)	0.524	0.570	0.578	0.622	0.647
1984 - 1995 (V)	0.496	0.516	0.525	0.607	0.546
1951 - 1961 (V)	0.433	0.568	0.458	0.660	0.572

**Figure 18: Nash-Sutcliffe Efficiency of ACS- based model and benchmark model, all zonal parameters coupled**

Section of model performance has been extended to include the presented results, *Page 18, Line 15*:

“A high number of parameters is assumed to offer a model structure with a higher flexibility to match the observed data, though its higher complexity might lower its performance. To compare our proposed model structure with a benchmark at a similar number of parameters we added a third calibration strategy. The performed approach coupled all zonal parameters as described above. This lowered the amount of parameters per sub-basin to 45 for both model setups. As it can be seen in Tab. 4 the total amount of parameters in the benchmark partition is higher than in the new ACS-based partition.

After the calibration (time period 1995-2006) we evaluated the model’s performance in three validation periods. Two in direct (temporal) neighbourhood to the calibration period and the last at the very beginning of the time series. Model performance has been calculated as the average Nash-Sutcliffe-Efficiency (NSE) (Nash and Sutcliffe, 1970) of all gauges and is tabulated in Tab. 5. Results show that

ACS-parametrisations are superior in all cases. Its increase in performance ranges from 17-52% in comparison to the free-, 11-21% to the 6-parameter-coupled benchmark and 5-19% to the all-coupled parametrisation.

Beside this “lumped” evaluation we compared the performance of the models at each gauge in each period. A comparison of NSE for 6-parameter coupled model is shown in Fig. 16, for ACS and free-benchmark model in Fig. 17. Comparison for the all-coupled parametrisation is shown in Fig. 18. We can see that the individual performances led to the same conclusion as the lumped performance, though some results are better for benchmark models (both parametrisations). To be more precise, in case of 6-parameter coupled model 20 points (rep. a single gauge in one of the time periods) are below equivalency (rep. a better performance of the benchmark model), in case of the free-benchmark model 12 and for the all-coupled benchmark 23 points. Representing 15%, 9% and 20% of the evaluated cases.

## Response to Reviewer Comment #2

Response to outlined problems:

1. “First problem is that some basic mathematics is unclear, e.g. eqs. (1) and (2). The summation variable in (1) needs clarification.  $x$  is running from  $i \cdot \Delta s$  to  $(i+1) \cdot \Delta s$ , but there is no indication of the range of  $x$ -values to be applied. In (1) the mean value  $E(C)_i$  is established, but in the calculation of the standard deviation in (2) the applied mean value is denoted  $E(C)_x$ ”

We agree on this point. The formulation has been not correctly. We propose the following revision for page 6, after line 5:

“The stream flow length was subdivided into multiples of the length  $\Delta s$  (for  $x_S$ ) and the hillslope flow length subdivided into multiples of the distances  $\Delta o$  (for  $x_H$ ). Distance classes defined in this way will split the basin into stripes. Depending on the width  $\Delta s$  the basin would be classified into  $N_S$  distance classes, where  $N_S$  is an integer larger or equal to one.

Let us now look at a single distance class  $i$ , where  $i$  indicates the class. All cells of the input data with a flow distance in a range between  $i \cdot \Delta s$  and  $(i+1) \cdot \Delta s$  are assigned to this distance class. We can write the set of distances of  $x_S$  assigned to  $i$  as the following set  $B$ :

$$B = [i \cdot \Delta s; (i+1) \cdot \Delta s] \quad (1)$$

To characterise a property  $C$  in the distance class  $i$  we can calculate the expected value  $E(C)$  and standard deviation  $\sigma(C)$ , taking only those values of  $C$  into account that are situated in the boundaries of the distance classes:

$$E(C)_i = \frac{1}{w(i \cdot \Delta s)} \sum_{(j|x_{S,j} \in B)} C_j \quad (2) \quad \text{and} \quad \sigma(C)_i = \sqrt{\frac{1}{w(i \cdot \Delta s)} \sum_{(j|x_{S,j} \in B)} (C_j - E(C)_i)^2} \quad (3)$$

$w(i \cdot \Delta s)$  represents the number of values (or grid cells) within the class. Please note that  $w(x)$  is the non-normalised value of the area-function (Snell and Sivapalan, 1994).”,



To enhance index consistency we changed the following equation:

Page 6, line 15, Eq. 3:	Index j replaced with i, indicating distance class numbers
Page 7, line 20, Eq. 4 & line 23, Eq. 5	Index j replaced with i, indicating distance class numbers
Page 10, line 9, Eq. 7	Index j replaced with b, indicating parallel basins/zones *

\* required further changes in the manuscript after line 10:

“with  $P_i$  being the number of parallel basins or zones,  $w(i \cdot \Delta s)_p$  the number of cells within the distance-class  $i$  of the considered parallel basin/zone  $b$  and  $\sigma(C)_{i;p}$  being the neighbouring standard deviations”

2. “Second problem is the awkward English, which is below an acceptable standard for a high quality journal. There are numerous grammatical errors (punctuation; wrong tense, wrong words, missing words, bad construction of sentences etc.), which is very disturbing for grasping the real content of the paper.”

Your comment on linguistic quality and/or style has been stated by the first referee as well. To comply with the standard of the journal the manuscript is underwent extensive linguistic revision. Again, the result of linguistic revision can be seen below.

### Response to Reviewer Comment #3

Your first point has been stated by all reviewers so far and we truly accept this critique. Results of this revision, again, can be tracked below.

The second point intersects with the readability. You suggest a more technical, mathematical description of the algorithm. In the former submission of this manuscript we focused on a technical description of the algorithm and its functionality (but based on the reviews we decided to withdraw the manuscript and focus more on modelling application). A major point of the revisions for the previous manuscript was a too technical depiction of the algorithm that did not match the requirements of a research paper. Hence, we omitted the detailed description and offered a “verbose” qualitative description. We added the appendix to show the functionality of the involved tools. In its actual form, the manuscript is intended to offer a trade-off between technical detail and facile qualitative description.

Nevertheless, the sequence of the algorithm is shown and described in the manuscript. For readers with more interest in the algorithm and its implementation we made the code available as supplementary to this paper.

Besides the structure of the paper, you pointed out that the background of the threshold  $\Omega$  and the non-linearity coefficient  $e$  is not made clear.

As described in Sect. 3.2.1 the threshold  $\Omega$  is used to distinguish between distance classes comprising “high” and “low” variance. Since we do not know the exact amount of tolerable variance we had to come up with a concept to value our target. There are several ways to do so. One way might be to just take an arbitrary percentile of present variance, a valuation by cluster analysis or by setting it to a fixed number.

But the threshold, and hence the number of ascertained sub-basins, is dependent on the purpose of the performed partition. For some applications a detailed subdivision, bringing the heterogeneity to a minimum (will result in

more computational effort), might be desirable while for other purposes a facile partition might be sufficient. We intended to implement a flexible function that unites the requirements for both purposes (and in between).

The weighting factor  $\omega$  offers this kind of flexibility and  $e$  is its parameter. If  $e$  tends to zero, the threshold  $\Omega$  tends to the average of present standard deviation. The factor  $e$  set to this value should be used in applications where only regions with significantly higher heterogeneity are to be captured. If  $e$  increases the threshold lowers and hence the number of subdivisions is likely to increase. With an increasing factor  $e$  more heterogeneity is captured by the algorithm.

Though it is interesting which value for  $e$  is suitable for what kind of application we omitted deliberately a detailed analysis. In the present state of the manuscript  $e$  is a user-dependent specification and its introduction aims to lower the range of possible arbitrary threshold values. In the following figure Fig. RC1 we compared the value of  $\Omega$  to percentiles of present standard deviation values in the Mulde catchment. As it can be seen we approximately bisect the range of possible values. All figures in the manuscript involving  $\Omega$  use three different values of  $e$ , namely 0., 0.5 and 1. Our intention was to show a possible range of  $\Omega$  in our application, though we constantly set  $e = 0.5$ . All this is indeed missing in the manuscript because we ascribed only minor importance on this factor.

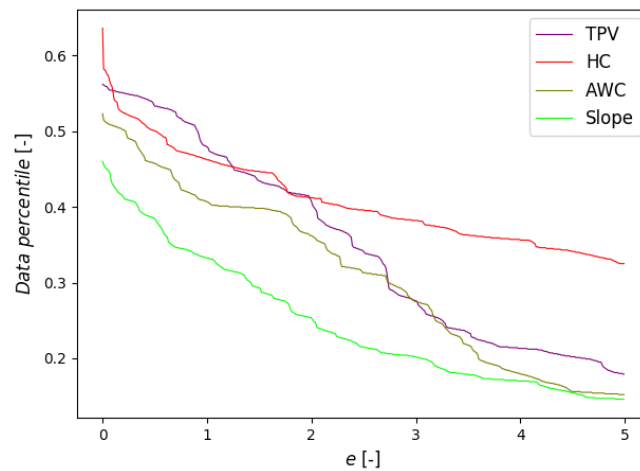


**Figure RC1: Percentile of  $\Omega$  against non-linearity factor  $e$**

To make the concept of the non-linearity factor  $e$ , its chosen value in the application and its constant depiction in the distance-factor functions understandable we added the following lines on page 8, line 4:

“As the index  $N_s$  in Eq. (3) indicates, the threshold  $\Omega$  is calculated for the entire catchment and does not necessarily represent the true value of  $\sigma(C)$  for homogeneous sub-basins. It just helps to distinguish regions of high and low variances. Therefore it is recommended to vary the value of the non-linearity factor  $e$  in a range of  $[0; \infty]$ , though values between 0 and 1 were found most applicable in our case studies. If  $e$  is set to zero  $\Omega$  is equal to the average of  $\sigma(C)$  in the basin. As  $e$  is increased  $\Omega$  lowers. The choice of  $e$  is dependent on the intention of the purpose of partition. If a detailed subdivision is required to capture the majority of heterogeneity  $e$  should be set to value greater or equal to 1. Otherwise if only regions with a significantly higher heterogeneity are to be captured  $e$  is recommended to be set to 0. However, in the presented case studies  $e$  has been set to 0.5. To indicate the range of potential results  $\Omega$  is shown in all distance-factor functions for values of  $e \sim 0., 0.5$  and 1.0.”

To your last sub-point of your critique on the depiction of the algorithm we would like to give a detailed response. The revision of mathematical equations has been pursued from the response to Comment #2 as follows:

We introduced a set  $B$  of stream-flow distances  $x_s$  to the description of the distance-factor function (Page 6, Line 12):

$$B = [i \cdot \Delta s; (i+1) \cdot \Delta s] \quad (1)$$

The variable  $i$  is an integer ranging from 1 to  $N_s$ , the number of distance classes in the basin.

This set is used afterwards in the equations for  $E(C)$  and  $\sigma(C)$ :

$$E(C)_i = \frac{1}{w(i \cdot \Delta s)} \sum_{(j|x_{s,j} \in B)} C_j \quad (2)$$

$$\sigma(C)_i = \sqrt{\frac{1}{w(i \cdot \Delta s)} \sum_{(j|x_{s,j} \in B)} (C_j - E(C)_i)^2} \quad (3)$$

Equation 3 (now 4), [Page 7, line 20] the beforehand discussed threshold  $\Omega$ , had also not been compiled correctly. As you pointed out the factor  $e$  has to appear in the nominator and denominator:

$$\Omega = \frac{\sum_{i=1}^{N_s} \omega_i^e \cdot \sigma(C)_i}{\sum_{i=1}^{N_s} \omega_i^e} \quad (4)$$

Furthermore, the weighting factor Eq. 4 (now 5) on page 7, line 23, has been changed to make the range of Min/Max Function clear:

$$\omega_i = \frac{\sigma(C)_i - \max_{1 \leq i \leq N_s} (\sigma(C)_i)}{\min_{1 \leq i \leq N_s} (\sigma(C)_i) - \max_{1 \leq i \leq N_s} (\sigma(C)_i)} \quad (5)$$

The objective function Eq. 5 (now 6) has been updated analogously [Page 7, line 26]:

$$Z = \left[ [i \mid 0 \leq i \leq N_s; \sigma(C)_i > \Omega] \right] \rightarrow \min \quad (6)$$

On page 9, line 9, Eq.6 (now 7) the evaluation scheme has been updated as well. We added a new index  $p$  to denote parallel sub-basins (We changed the index character to prevent a mistake with the set  $B$  (Eq. 1)). Index  $p$  is an integer ranging from 1 to  $P_i$ , the number of parallel sub-basins within the original basin  $i$  ( $i \in [0; N_s]$ ). Remaining indices have been matched with the general notations:

$$\sigma_s(C)_i = \frac{1}{\sum_{p=1}^{P_i} w(i \cdot \Delta s)_p} \cdot \sum_{p=1}^{P_i} \sigma(C)_{i,p} \cdot w(i \cdot \Delta s)_p \quad (7)$$

Your last comment addresses the model application. You suggest to substitute the NSE-based calibration study with a parameter uncertainty analysis or to omit the model application.

Likewise to your critique of the manuscript structure and algorithm depiction we shared your opinion. Moreover the previous submission of the paper changed our attitude. While the detailed technical description was heavily criticised in the previous manuscript, the missing model application “where a model with the new subdivision

outperforms another model” was strongly recommended. So (again) this chapter has been incorporated to meet such expectations. A reduction to the variance topic would be contrary to the aims of this manuscript, defined in the introduction (and title), that clearly sets for modelling purposes. Since we expected that many readers would ask for that missing modelling aspect we would like to keep this section in the manuscript.

Nevertheless, our main intention is to present the method, its ability to capture catchment heterogeneity and the insights on catchment organisation. This is why we only performed a short and simple modelling study with 3 (now 5, see Response to reviewer comment #1) calibrated model setups.

The problem with NSE-based comparisons is indeed their dependence on the applied calibration procedure. Therefore, we tried to apply the same calibration strategy to both spatial setups, titled “coupled” calibration for ACS and the benchmark setup. In both applications the same 6 parameters are coupled and the identical calibration tool and the same number of iterations has been used. The only thing changed is the coupling-information, the land cover in the benchmark setup and TPV-values in the ACS setup. This procedure is described on *page 17 from line 27 to page 18, line 9*.

Additionally, we allowed the benchmark setup to exploit its full number of parameters in an unconstrained calibration run, involving the same calibration tool and number of iterations (as described from line 7 to 9). As reviewer #1 pointed out we had a parameter mismatch in this calibration study and we therefore introduced a second parameter coupling applied to all zonal-parameters. The results and changes in manuscript can be found in our response to the first reviewer.

Your suggestion on parameter uncertainty seems quite appealing, though. Therefore, we performed a Monte-Carlo Simulation with 10'000 random parameterisations and saved the resulting NSE and parameters for several sub-basin in the Mulde catchment. The Monte-Carlo simulation has been applied to the all-parameter coupling scheme. We evaluated our results scantily with a GLUE approach. We used the NSE as generalised likelihood function and set a threshold of 1% for behavioural parameter sets. Parameter uncertainty has been calculated with the following equation:

$$U(Par) = \sqrt{\frac{\sum_{x \in Nx} (Par_x - \bar{P})^2 \cdot NSE_x}{\sum_{x \in Nx} NSE_x}}$$

where  $Par$  is the analysed parameter,  $Nx$  is the behavioural parameter set,  $NSE_x$  is the generalised likelihood of the parameter set and  $\bar{P}$  the average parameter in set  $Nx$ :

$$\bar{P} = \frac{1}{|Nx|} \cdot \sum_{x \in Nx} Par_x$$

To compare the uncertainty of all parameters their actual values have been normalised by their parameter constraints. In Tab. RC2 all parameters are given with their lower and upper boundaries, grouped by their usage in the model. “Single” parameters are used in the ground water levels and post-processing of the model, “Coupled” parameters are used in each individual zone. Since we applied the all-parameter coupling scheme, these parameters are estimated once per sub-basin and by a linear coupling coefficient transferred to all zones (See response to Comment #1). The coupling parameters are not shown in Tab. RC2 but their values are uniformly in the interval [0, 2].

**Table RC2: Parameter constraints HBV<sub>96</sub> model**

Parameter	Lower Boundary	Upper Boundary
<b>Single</b>		
ALPHA	0	2
K4	0.001	0.5
KHQ	0.01	0.5
PERC MAX	0	5
MAXBAZ	0	1
<b>Coupled</b>		
BETA	1	4
CFLUX	0	2
CFMAX	1	6
CFR	0	2
DTM	-2	2
ECORR	0.95	1.05
EPF	0	0.2
ERED	0	0.5
ETF	0	0.2
FC	100	500
ICMAX	1	20
LP	0.75	1
RFCF	0.95	1.05
SFCF	0.95	1.05
TT	-2	2
TTINT	1	5
WHC	0	2

Following figures RC3-6 we plot  $\bar{P}$  in the normalised parameter space for ACS setup and the benchmark setup for a single sub-basin, where the shown error bars represent calculated  $U(Par)$  values.

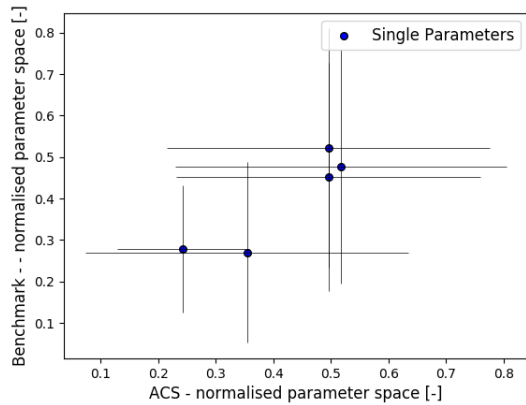


**Figure RC3: Single parameters**

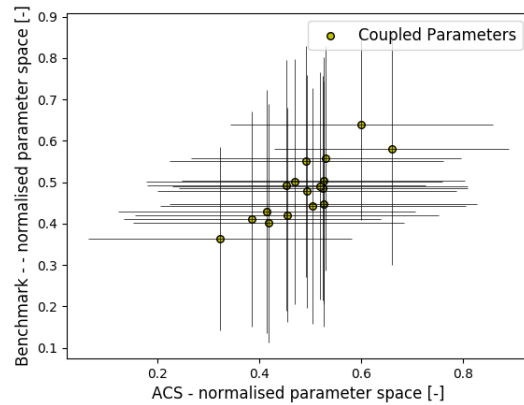


**Figure RC4: Coupled parameters**

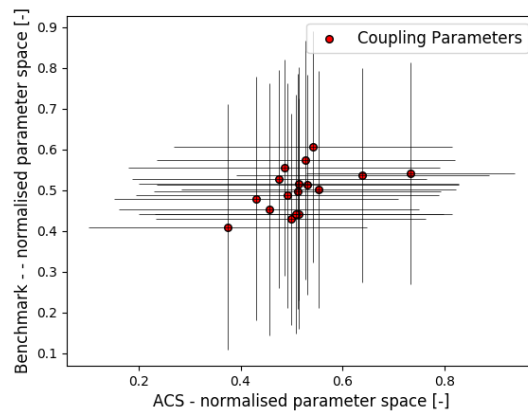
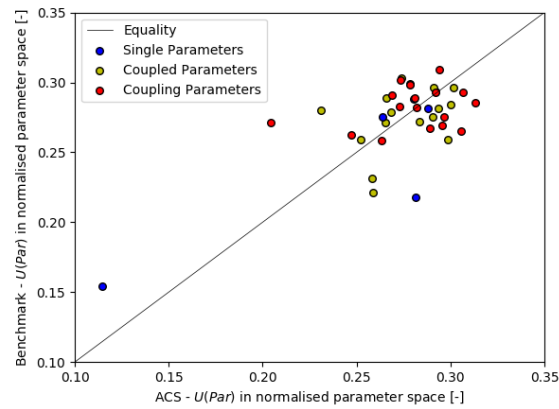


**Figure RC5: Coupling parameters**

As it can be seen in the figures above the uncertainty indicators are symmetrical for the most parameters, meaning that the uncertainty is equal for both models. Uncertainty values for the benchmark and ACS setup plotted against each other are given in the following Fig. RC6:



In Fig. RC6 several points are located above the “Equality” line, meaning that parameter uncertainty for an individual parameter is higher for the benchmark model than for ACS-model. But nearly the same number is below the line.

These results indicate that the parameter uncertainty could not be lowered (significantly). But this is only a fast and simple evaluation and its result might change with an elaborate technique.

Considering the length of the manuscript we preferred not to include these results (or similar) in the paper, because its explanation (method, model, parameters, etc.) would effort a lot of additional information that are irrelevant for the ACS algorithm.